Ultrafast Dynamics of the Azobenzene−Coumarin Complex: Investigation of Cooling Dynamics Measured by an Integrated Molecular Thermometer

Suresh Velate, Evgeny O. Danilov,* and Michael A. J. Rodgers

Department of Chemistry and Center for Photochemical Sciences, 141 Overman Hall, Bowling Green State University, Bowling Green, Ohio 43403

Received: May 12, 2005; In Final Form: August 9, 2005

The energy dissipation mechanism from photoexcited azobenzene (Az) was studied by femtosecond time-resolved UV absorption spectroscopy using 7-amino-4-trifluoromethylcoumarin (ATC) as a probe. The distance between the probe molecule and Az was fixed by covalently linking them together through a rigid proline spacer. Picosecond dynamics in THF solutions were studied upon excitation into the S_1 state by a 100 fs laser pulse at 480 nm. Transient absorption spectra obtained for Az-Pro-ATC combined the S_1 state absorption and vibrationally excited ground-state absorption of ATC. Correction of the transient spectrum of Az-Pro-ATC for the S_1 absorption provided the time-resolved absorption spectrum of the ATC hot band. Three major components were observed in the transient kinetics of Az-Pro-ATC vibrational cooling. It is proposed that in ca. 0.25 ps after the excitation, the S_1 state of azobenzene decays to form an initial vibrationally excited nonthermalized ground state of Az-Pro-ATC that involves vibrational modes of both azobenzene and coumarin. This hot ground state decays in ca. 0.32 ps to the next, vibrationally equilibrated, transient state by redistributing the energy within the molecule. Subsequently, the latter state cools by transferring its energy to the closest solvent molecules in ca. 5 ps; then, the energy diffuses to the bulk solvent in 13 ps.

1. Introduction

Nonradiative energy dissipation mechanisms from the excited states of molecules in solution have been a subject of interest for decades.[1−6] The rapid deactivation of electronic states via nonradiative channels results in energy transfer to the matrix species around the chromophore, thereby heating the local environment. In a simplified picture this process of energy transfer from the chromophore to the surroundings can be explained in two steps: (i) fast intramolecular vibrational redistribution over all vibrational modes of the molecule and (ii) intermolecular energy transfer of vibrational energy from the molecule to the surrounding matrix. Sophisticated experimental techniques exploiting ultrashort IR pulses have been employed in recent years to monitor such energy transfer processes,[7−13] but useful knowledge can also be gained in the visible spectral region. Most of the experiments in the visible region have been performed by ultrafast spectrometric techniques[6] where the vibrational cooling of a photoexcited molecule is monitored either as change in transient absorption[14−17] or in fluorescence.[17]

In most of the experiments reported so far intramolecular energy redistribution in dye molecules has been investigated by using the slope of the low-energy edge of its electronic transitions. Gottfried et al. have reported rapid intramolecular redistribution of the vibrational energy of anthracene and coumarin in solutions by these methods.[2] An alternative way to investigate this process is to use a probe molecule (a molecular thermometer) that is not excited initially but rather senses the passage of thermal energy dissipating from the light-absorbing species (the heater). Further development of this idea has led to the introduction of the concept of a molecular heater−thermometer integrated system where two different molecules, namely, a heater that absorbs the visible radiation, and a thermometer that probes the temperature by changing the absorption in the vicinity of its hot band, are brought into proximity by covalently linking the two discrete molecules.[18,19]

Azobenzene and its derivatives are good candidates for many applications such as light-triggered switches,[20] constituents of erasable holographic data image storage devices, and materials whose physical properties can be modulated by light.[21−24] Such compounds have been studied extensively by steady-state spectrometric and photochemical methods including UV−vis absorption,[25,26] Raman,[27] NMR,[28] and by theoretical modeling.[29−31] The mechanism of trans−cis isomerization in azobenzene and its excited state dynamics have attracted considerable attention. However, there have been relatively few time-resolved studies of azobenzene photochemistry,[32,33] especially concerning nonradiative energy dissipation in azobenzene.[34−37]

In this work, we have studied the mechanism of thermal dissipation in and from the azobenzene molecule. With the use of ultrafast UV−vis pump−probe spectrometry, energy transfer in the photoexcited molecule has been measured with a molecular thermometer linked to the azobenzene moiety through a rigid proline spacer (Figure 1). The experimental observations were compared with those from an azobenzene model compound.

2. Experimental Section

2.1. Instrumentation. The laser system and pump−probe spectrograph for the ultrafast transient absorption experiments have been described elsewhere.[37] Briefly, the 800 nm output of a mode-locked, Ti:Sapphire laser (Hurricane, Spectra-Physics) was typically 1.0 mJ/pulse (fwhm < 100 fs) at a repetition rate of 1 kHz. The output of the laser was either steered into a

* Corresponding author. Phone: (419) 372-9311. Fax: (419) 372-9300. E-mail: danilov@bgnet.bgsu.edu.

10.1021/jp052501i CCC: $30.25
Published on Web 09/16/2005

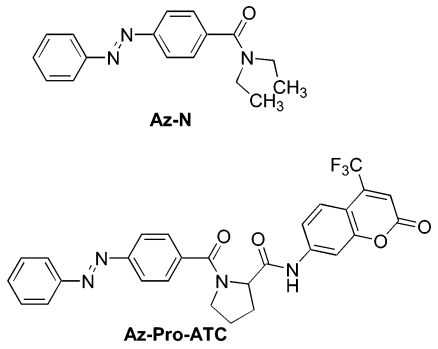

Figure 1. The structure of the compounds studied.

second- or third-harmonic generator (Super Tripler, CSK) or into an optical parametric amplifier (OPA 800C, Spectra-Physics) to produce pulses at 483 nm; 85% of the amplifier output was used to generate the pump pulses while 8% was used for white light generation. The white light continuum generation was accomplished by focusing the fundamental (800 nm) into a CaF_2 crystal.

Prior to generating the probe continuum, the probe beam at 800 nm was passed through a delay line (MM 4000, Newport), which provided an experimental time window of 1.6 ns with a step resolution of 6.6 fs. The energy of the probe pulses was $<0.5\ \mu J$ at the sample. An optical chopper was used to modulate the excitation beam in order to switch the sample between excited and ground states at a frequency of 100 Hz. The angle between the pump and the probe beam was approx 6°. The sample cell had an optical path of 2 mm. After the sample cell, the continuum was coupled into a 400 μm diameter optical fiber and thereafter input into the CCD spectrograph (Ocean Optics, S2000 or Control Development) for time-resolved spectral information (350−800 nm).

In a typical experiment, 5000 excitation pulses were employed to obtain an averaged transient spectrum at a particular delay line setting. The CCD spectrograph and the delay line were computer-controlled. In-house LabVIEW (National Instruments) software routines allowed automatic spectral acquisition over a series of delay settings. Kinetic traces at appropriate wavelengths were assembled from the accumulated spectral data. The rise time of the spectrometer was ca. 120 fs. The sample solutions were prepared to have an absorbance of 0.2−0.3 AU at the excitation wavelength in the 2 mm cuvette. The absorption spectra of the solutions were measured before and after the experiment to check for possible sample decomposition.

Ground-state absorption spectra were recorded on a single-beam Varian Cary 50 Bio spectrophotometer. Nuclear magnetic resonance (NMR) spectra were recorded on 200 (Varian Gemini-200) or 400 MHz (Varian Unity Plus) spectrometers. $CDCl_3$ was the solvent for NMR unless otherwise noted, and chemical shifts are reported in parts per million (ppm) for ^{1}H NMR on the δ scale relative to TMS at 0.0 ppm. GC/MS and DIP/MS were collected on an HP 5988 mass spectrometer coupled to an HP 5880A GC with a 30 m × 0.25 mm × 0.25 μm column.

2.2. Materials. Tetrahydrofuran (Aldrich 99.8%) was used as received. Azobenzene carboxylic acid, 7-amino-4-trifluoromethylcoumarin (ATC), and *N,N*-diethylamine were obtained from Aldrich and were used without further purification. All reagents and solvents were obtained from commercial suppliers and used as received unless otherwise noted. Pyridine was dried over potassium hydroxide and distilled off as required.

2.3. Synthesis. *2.3.1. Synthesis of Az-Pro-ATC.* Azobenzoyl chloride (1.95 g, 8 mmol) was mixed with proline methyl ester (1 g, 7.8 mmol) in pyridine (10 mL) and heated at 60 °C for 24 h. After 24 h the reaction mixture was cooled and neutralized with dilute hydrochloric acid. The precipitated compound was filtered and redissolved in dichloromethane. It was washed with sodium hydrogen carbonate solution and then water. The solution was dried over sodium sulfate and purified by column chromatograpy on silica gel using a mixture (1:20) of ethyl acetate and hexane as solvent to yield 1.4 g (4.15 mmol) of *N*-azobenzoyl proline methyl ester. ^{1}H NMR (200 MHz, $CDCl_3$) δ: 7.95 (t, C−H aromatic, 4H), 7.7 (d, C−H aromatic, 2H), 7.45 (m, C−H aromatic, 3H), 4.7 (t, C−H proline, 1H), 3.9 (s, O−CH_3, 3H), 3.75 (m, −CH_2−, 1H), 3.45 (t, −CH_2−, 1H), 1.9−2.2 (m, −CH_2−CH_2−, 4H). MS (EI): 337, 278, 232, 209, 145, 104, 77, 51.

A volume of 10 mL of sodium hydroxide (10%) in water was added to a solution of *N*-azobenzoyl proline methyl ester in methanol, and the mixture was stirred for 10 h. The methanol was evaporated under reduced pressure, and the aqueous phase was washed with diethyl ether, acidified with 1 M hydrochloric acid to pH 3−4, and extracted with ethyl acetate. Organic fractions were combined and dried over sodium sulfate. Excess solvent was removed under reduced pressure to give 1.1 g (3.4 mmol) of *N*-azobenzoyl proline. ^{1}H NMR (400 MHz, $CDCl_3$) δ: 8.0 (t, C−H aromatic, 4H), 7.75 (d, C−H aromatic, 2H), 7.5 (m, C−H aromatic, 3H), 4.8 (t, C−H proline, 1H), 3.6 (m, −CH_2−, 2H), 2.45 (q, −CH_2−, 1H), 2.25 (q, −CH_2−, 1H), 2.1 (q, −CH_2−, 1H), 1.95(q, −CH_2−, 1H).

To an ice cold solution of ethyl chloroformate(0.5 mL, 5.2 mmol) in THF, the above precipitate (1 g, 3.1 mmol) in tetrahydrofuran (10 mL) and triethylamine (0.4 mL) was added dropwise and stirred for 10 min. To this solution amino methyl coumarin (700 mg, 3.1 mmol) in THF (8 mL), which further contains triethylamine, was added in 30 min at ice cold temperature. It was then stirred for 30 min more at 0 °C and then allowed to warm to room temperature. It was then stirred at room temperature for 30 min and then at 50 °C for 8 h. Tetrahydrofuran was removed under reduced pressure. The crude product was then redissolved in dichloromethane and washed with water, dilute hydrochloric acid, sodium hydrogen carbonate, and again with water. The dichloromethane layer was then dried over anhydrous sodium sulfate, and the excess solvent was removed under reduced pressure. The product was further purified by column chromatography using a mixture of hexane and ethyl acetate as solvent to give Az-Pro-ATC. ^{1}HNMR (400 MHz, $CDCl_3$) δ: 10.2 (s, −CO−NH− 1H), 7.7 (d, C−H aromatic, 1 H), 7.2−7.4 (m, C−H aromatic, 11H) 6.7 (s, C−H, 1H), 5.05 (m, C−H, proline), 3.6 (m, −N−CH_2−, 2H), 1.95−2.3 (m, −CH_2−CH_2−, 4H). ^{13}C NMR (400 MHz, $CDCl_3$) δ: 171.63, 167.73, 158.87, 154.96, 152.63, 143.57, 139,63, 138.83, 132.2, 129.78, 128.72, 128.03, 125.66, 122.934, 122.68, 122.17, 120.28, 116.29, 114.67, 108.47, 106.45, 63.85, 51.32, 26.78, 26.1. MS (EI): 534.

2.3.2. Synthesis of AzN. The model compound Az-N was prepared by heating a mixture of azobenozyl chloride (1 g, 4.1mmol) and diethylamine (0.6 g, 8.2 mmol) in pyridine (10 mL) for 10 h at 60 °C. After 10 h the reaction mixture was cooled and neutralized with dilute hydrochloric acid. The precipitated compound was filtered and redissolved in dichloromethane. It was then washed with sodium hydrogen carbonate solution and then water. The solution was dried over sodium sulfate. Dichloromethane was removed under reduced pressure to give 0.7 g of Az-N. ^{1}H NMR (200 MHz, $CDCl_3$) δ: 7.95 (m, −CH− aromatic, 4H), 7.5 (m, −CH−aromatic, 5H), 3.6 (−N−CH_2, 2H), 3.3 (−N−CH_2, 2H), 1.3 (−CH_3, 3H), 1.15 (−CH_3, 3H). MS (EI): 281.

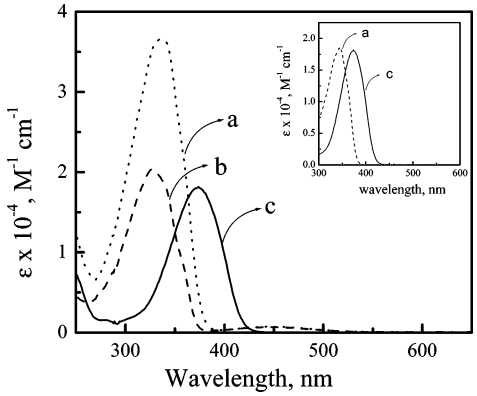

Figure 2. Ground-state absorption spectrum of Az-Pro-ATC (a), Az-N (b), and ATC (c). The inset shows the spectrum of Az-Pro-ATC (a) corrected for the ground-state absorption of azobenzene compared with a directly measured spectrum of ATC (c).

2.4. Computations. All calculations were performed using the Gaussian 98 package[38] with a 6-31G(d) basis set. Geometry optimization for the ground state was carried out with the B3LYP exchange correlation function.[39,40] This consists of the Lee−Yang−Parr correlation functional[40] in conjunction with the Becke hybrid exchange functional.[39] The latter is a linear combination of the local density approximation, Becke's gradient correlation,[41] and the Hartree−Fock exchange energy based on Kohn−Sham orbitals.[42] Energies and densities were obtained through the resolution of the Kohn−Sham equation using the B3LYP functional. Excitation energies were calculated using the TD−DFT implementation in Gaussian.

3. Results

3.1. Ground-State Absorption Spectrometry. The structures of Az-Pro-ATC and Az-N employed in this work are shown in Figure 1. Figure 2 shows the ground-state absorption spectra of these compounds in tetrahydrofuran. The lowest electronic transitions of Az-Pro-ATC and Az-N are an n−π* transition centered around 450 nm and a $\pi-\pi$* transition centered around 330 nm. While the n−π* transition is symmetry forbidden (ϵ = 700 M^{-1} cm^{-1} at 450 nm), the $\pi-\pi$* transition is strong (ϵ_{Az-N} = 20 215 M^{-1} cm^{-1} and $\epsilon_{Az-Pro-ATC}$ = 36 488 M^{-1} cm^{-1} at 330 nm). The ground-state spectrum of Az-Pro-ATC, subtracted for the ground-state absorption of azobenzene, was almost identical to the steady-state absorption spectrum of ATC in shape but shifted toward shorter wavelengths by ca. 50 nm (Figure 2, inset). It is evident from the difference absorption spectra that substitution of hydrogen on azobenzene with a prolyl group does not significantly change the electronic structure of azobenzene. The blue shift observed for the corrected spectrum of Az-Pro-ATC can be explained by the presence of an electron-withdrawing group on the amino group of ATC.

3.2. Molecular Orbitals Calculations. Optimized structures and molecular orbitals for Az-Pro-ATC from the Gaussian calculation are shown in Figure 3. The HOMO and LUMO are localized on the azobenzene moiety, whereas HOMO − 1 and LUMO + 1 are predominantly on the ATC moiety. On the basis of the TD−DFT calculation, the electronic transition of Az-Pro-ATC into the S_1 excited state can be assigned to a $HOMO_{Az} \rightarrow LUMO_{Az}$ transition, and transition into the S_2 state is associated with the $(HOMO - 2)_{Az} \rightarrow LUMO_{Az,}$ $(HOMO - 1)_{ATC} \rightarrow (LUMO + 1)_{ATC}$, and $(HOMO - 1)_{ATC} \rightarrow LUMO_{Az}$ transitions. The choice of the excitation wavelength (483 nm, vide infra) rules out the possibility of exciting S_2 transitions. Also, since there is no absorption band in the ground-state absorption spectrum of ATC near 483 nm, and therefore the direct excitation of ATC is not possible at the excitation wavelength, the effect of the $(HOMO - 1)_{ATC} \rightarrow LUMO_{Az}$ can be neglected. The contribution of this transition is very weak when compared to those of the other two transitions indicating that there is only a negligible amount of overlap in the molecular orbitals of azobenzene and ATC.

3.3. Transient Absorption Studies. The transient absorption behavior of Az-Pro-ATC (2.65 mM) in tetrahydrofuran was investigated following a 100 fs excitation pulse at 483 nm. The excitation wavelength was chosen to be near the red edge of the n−π* transition, since (i) this wavelength will excite only Az and (ii) excitation of Az into its S_1(n−π*) state with relatively low excess energy above the electronic origin of ca. 560 nm will minimize the opportunity of significant vibrational cooling from the Franck−Condon state to the lowest S_1 state (S_1* → S_1). The selection of 483 nm seemed a reasonable compromise. On excitation of Az-Pro-ATC at 483 nm, transient absorption was observed over the range of 400−650 nm, comprising a strong band at 420 nm and a weaker band at 550 nm (Figure 4). The transient absorption spectrum observed for Az-Pro-ATC was similar to that reported for the $S_1 \rightarrow S_n$ transition in *trans*-azobenzene.[43] The time profile at 500 nm was found to fit well with a double-exponential decay giving the dominating component of 0.28 ps (>99%) and a very minor one of 2.9 ps. The decay time constants obtained from the fit

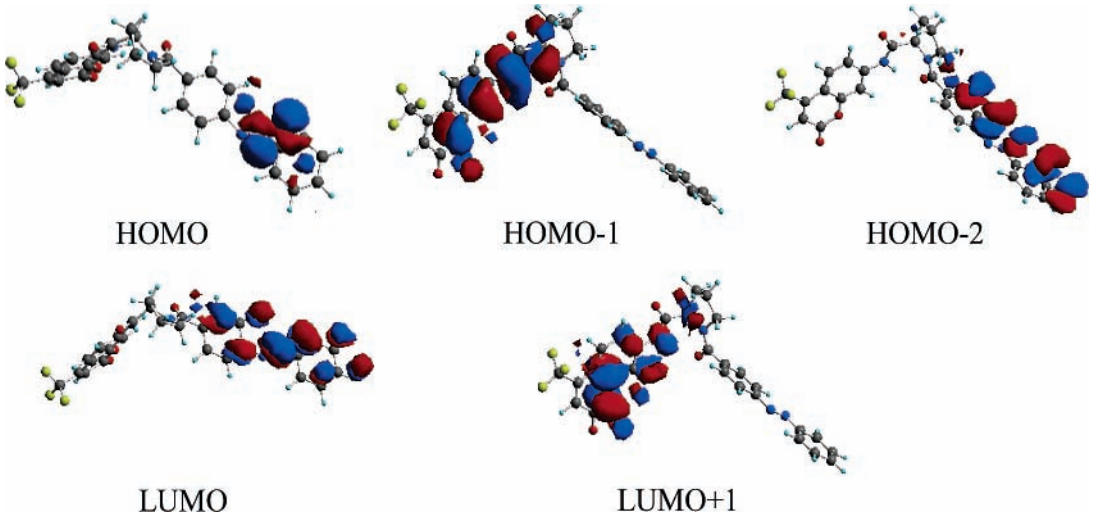

Figure 3. Molecular orbitals for the optimized ground-state structure of Az-Pro-ATC.

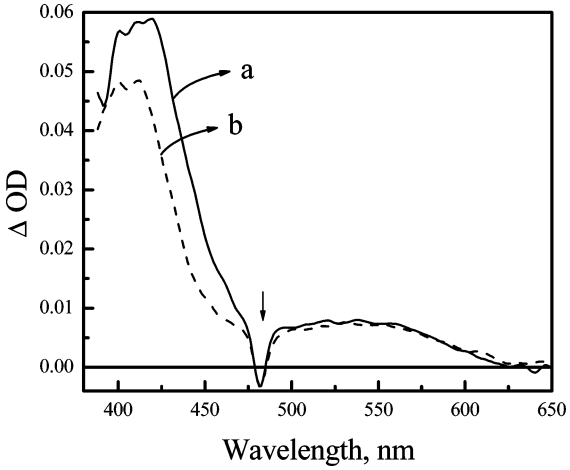

Figure 4. Transient absorption spectrum of (a) Az-Pro-ATC and (b) Az-N, obtained following the excitation of the azobenzene moiety at 483 nm. The arrow shows the wavelength of excitation.

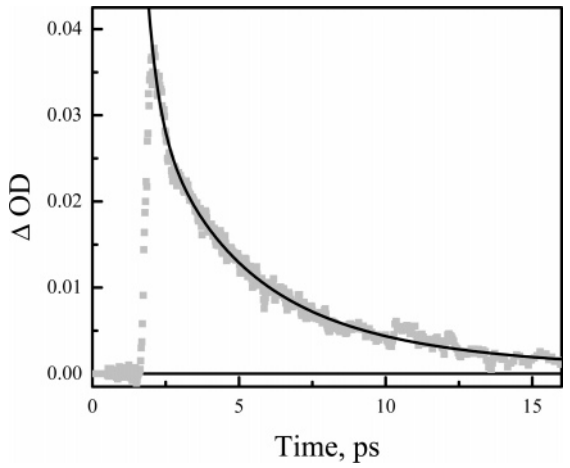

Figure 5. Decay profile of Az-Pro-ATC at 440 nm recorded immediately after the excitation of the azobenzene moiety at 483 nm. The solid line is the fit based on tetraexponential decay function with lifetimes of 0.32, 2.6, 5.2, and 13.5 ps.

at 550 nm gave 0.21 and 2.46 ps. Averaged over several wavelengths, the decay lifetimes are 0.25 ± 0.4 and 2.7 ± 0.2 ps. These observations agree with previously reported data,[43,44] where those decay times were assigned to the lifetime of the S_1 excited state with the shorter one associated with a direct departure from the initial Franck−Condon state and a direct descent on the S_1 potential surface toward a conical intersection, and the longer one associated with a diffusion-like motion on the S_1 surface.

The time profile at 440 nm was fitted with a four exponential function with lifetimes of $\tau_1 = 0.32$ ps, $\tau_2 = 2.6$ ps, $\tau_3 = 5.2$ ps, and $\tau_4 = 13.5$ ps (Figure 5). This indicates that the transient absorption spectrum obtained by excitation of Az-Pro-ATC at 483 nm is a mixture of the transient absorption spectrum of S_1 state of azobenzene with another absorbing species. One candidate for this entity is a transient enhancement of the ground-state hot band of the coumarin moiety.

4. Discussion

Figure 6 shows the result of correcting the transient absorption spectrum of Az-Pro-ATC for that of the S_1 excited state of azobenzene. The resulting spectrum had a range of 400−500 nm with a maximum around 430 nm. The transient absorption observed in the corrected spectrum of Az-Pro-ATC appears on

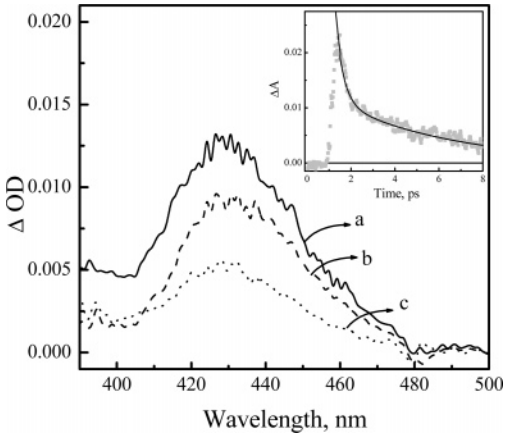

Figure 6. Transient absorption spectrum of Az-Pro-ATC corrected for the absorption of the singlet excited state of azobenzene at different time intervals: 2.0 ps (a), 3.5 ps (b), and 6 ps (c). The inset shows a time profile at 440 nm with the decay times of 0.32 and 5 ps.

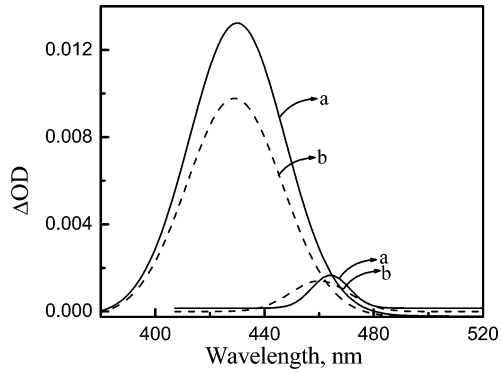

Figure 7. Representation of the corrected transient absorption obtained for Az-Pro-ATC as the sum of two Gaussian peaks at 2.0 ps (a) and 3.5 ps (b).

the red edge of the ground-state absorption of ATC. Since there is no direct excitation of ATC in Az-Pro-ATC, the formation of this band can be attributed to the hot band of ATC, which appears due to the thermal excitation into higher vibrational levels of the ground electronic state. The above observation can be further confirmed by resolving the corrected transient absorption spectrum into two bands, which might represent the vibrational progression of ATC with the spectral distance between the maxima corresponding to the lactone stretch (∼1722 cm^{-1}) or NHCO group (∼1625 cm^{-1}) vibrations (see, for instance, ref 45). As shown in Figure 7, the absorption spectrum can be fitted as the sum of two Gaussians. Curve a corresponds to the spectrum at 2 ps delay time. The large band on the blue side of the spectrum is centered at 430 nm (relative amplitude $A_{blue} = 0.0132$), and the smaller band has a maximum at 464 nm ($A_{red} = 0.001\,64$). At 3.5 ps (curve b), the larger band shifts to 428 nm ($A_{blue} = 0.009\,77$) and the smaller one to 460 nm ($A_{red} = 0.001\,40$). It was shown previously[46] that during the vibrational cooling of a rigid molecule having a high-frequency vibration, the ratio A_{blue}/A_{red} decreases with time. In our experiment A_{blue}/A_{red} at 2 ps is ∼8, and A_{blue}/A_{red} at 3.5 ps is ∼7. This result together with a small blue shift of the blue and red peaks and the narrowing of the overall band confirm the assignment of the corrected transient absorption spectrum to the hot band of ATC.

The time profile of this transient absorption at 440 nm revealed two major decay components of 0.32 and 5 ps (Figure 6, inset). There was also a contribution from a slower process in the transient kinetics, but the decay time constant could not

be decisively retrieved from the fit due to a poor signal-to-noise ratio. Additionally, the corrected transient signal grew in with a rise time constant that exceeded the time resolution of the system and was estimated as ca. 0.24 ps.

The decay of the transient absorption in Az-Pro-ATC at 440 nm indicated the presence of four discrete temporal processes. On the basis of the literature data,[43,44] the lifetimes of 0.25 and 2.7 ps can be assigned to the fast and delayed components of population decay of the S_1 state of azobenzene; the other processes observed in the transient kinetics must be due to the decay of the coumarin hot band. The 3-D transient absorption surface (in coordinates: time, wavelength, transient signal) corrected for the absorption of singlet excited state of azobenzene confirms this interpretation. The corrected transient spectrum is located in the wavelength range associated with the hot band absorption of coumarin.[18,19] It lacks the 0.25 and 2.7 ps components; instead, it has 0.32, 5.2, and 13.5 ps decay times and the rise time of 0.24 ps.

The hot band enhancement observed for ATC originates in the transient population of higher vibrational levels of the ground electronic state. This could arise by either of two possible energy transfer mechanisms: through-bond energy transfer (which can be regarded as intramolecular vibrational redistribution) and through-solvent energy transfer. The ratio between these two contributions depends on the effectiveness of heat transport along each pathway and can be characterized by the energy transfer parameters. It was shown previously[18,19,47,48] that in the case of weak thermal connection between the heater and the thermometer (when they are linked via a methylene group or both are just embedded in a matrix), the response registered by the molecular thermometer reflects the temperature of the heater's environment and contains a component that is relatively slow rising over time. This signal delayed with respect to the heating pulse was previously assigned to the intermolecular through-solvent heat transfer. On the other hand, in the case of a strong thermal connection between the heater and the thermometer, the thermometer's response would follow the cooling pattern of the heater loosing its thermal energy to the environment. The temperature recorded by the molecular thermometer will correspond to the temperature of the heater even though the thermometer is distanced from the heater by a few solvent shells and surrounded by the solvent molecules. The time dependence of the signal recorded by the molecular thermometer in this case would contain a decaying component rather than a rising one corresponding to intermolecular through-solvent heat transfer.

The transient absorption signal recorded in our experiment at 440 nm and then corrected for the S_1 excited state absorption of Az shows only one rise time, 0.24 ps, and no discernible rise component with a longer (ca. 15 ps) evolution time observed earlier in a number of solvents[33,35,36,44,46,49,50] and associated with the intermolecular through-solvent energy transfer from azobenzene. The rise time of 0.24 ps can be assigned to the lifetime of the S_1 excited state and the characteristic time of $S_1 \rightarrow S_0^*$ internal conversion. Another component of the S_1 lifetime, 2.6 ps, which also could be expected in the rise of the transient signal, could not be recognized due to its low relative contribution (<1%). Based on the kinetic behavior of the corrected transient signal at 440 nm, which we assign to the hot band of ATC, we adopt the model of strong thermal coupling between the heater (Az) and the thermometer (ATC). This idea is supported by recent theoretical work by Stratt and co-workers,[51−53] wherein the vibrational energy relaxation in liquids was studied. The model based on instantaneous-normal-mode

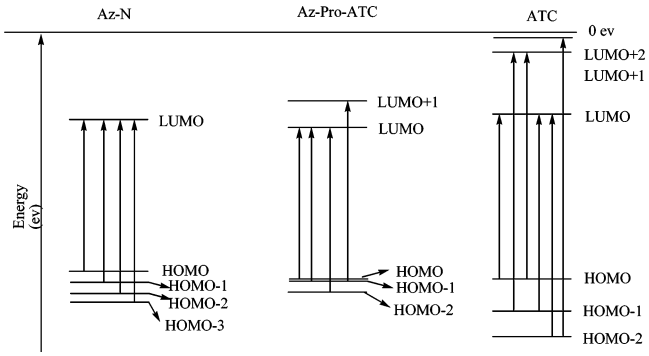

Figure 8. Schematic representation of the MO energy for Az-N, Az-Pro-C151, and ATC obtained from the calculations. The transitions shown in the picture are based on the results of TD−DFT calculations.

analysis assumed that a molecule loses energy as a result of solvent-assisted cascade events involving intramolecular vibrational energy redistribution (IVR) and a direct vibrational cooling. The calculations revealed that for a high-frequency mode the IVR rate might considerably exceed the rate of the direct vibrational cooling. It is therefore not surprising that vibrational energy redistribution between Az and ATC dominates in relaxation of the vibrational modes initially coupled with the excited electronic state. A possibility of the strong thermal coupling between Az and ATC is also supported by electronic energy level structure resulting from calculations. As shown in the diagram (Figure 8) in the case of Az-Pro-ATC, the energy gap between the HOMO and HOMO − 1 is very low. This low energy gap between the HOMO, which is localized on the azobenzene moiety, and HOMO − 1, which is localized on the coumarin moiety, could be the reason for the strong coupling between the higher vibrational levels of Az and ATC and the possibility of an effective energy transfer from vibrationally excited azobenzene to coumarin. In this picture, ca. 0.7 ps after the pump laser pulse at 483 nm, the decay of the S_1 excited state of Az creates an initial vibrationally excited nonthermalized ground state of Az-Pro-ATC that involves vibrational modes of both azobenzene and coumarin. This state cools in three steps having the decay times of 0.32, 5.2, and 13.5 ps being monitored by the hot band absorption of the coumarin moiety. Currently adopted models of vibrational cooling imply that internal conversion from the initially excited electronic state rapidly produces a ground state with highly excited high-frequency vibrational modes, and after internal vibrational energy redistribution this initial state cools via intermolecular interaction with a solvent.[46] In turn, this intermolecular process can proceed in two steps: first, the heat transfer to the immediate shell of the solute and then a slower heat diffusion to surrounding solvent.[19,46,54] Based on these models, we assign the fast decay time of 0.32 ps to the decay of the initial nonthermalized vibrationally excited state and the formation of equilibrated energy distribution within the Az-Pro-ATC vibrational manifold. The decay times of 5.2 and 13.5 ps can be assigned to the intermolecular heat transfer to the closest solvent shell having strong thermal coupling with the solute and a slower heat diffusion process from this shell to the bulk solvent, respectively. These results agree with previously published data on IR studies of electronically excited Az where intermolecular cooling took place in ca. 10−20 ps. The IR signal modulation with a characteristic time of 5−6 ps was also observed in the experiments.

To calibrate the coumarin molecular thermometer in temperature units, one has to establish a relationship between the change in optical absorption and the temperature. Kaiser and

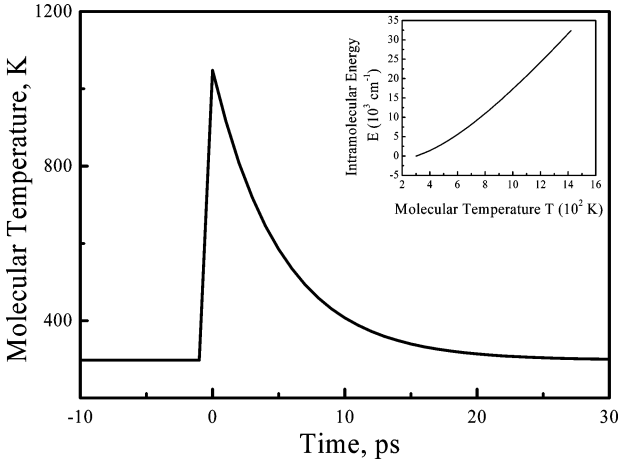

Figure 9. Analysis of the temperature change of ATC based on the time profile obtained for the decay of Az-Pro-ATC at 440 nm.

co-workers introduced the following equation for analyzing the temperature-dependent electronic absorption spectrum.[1,6,55] They expressed the frequency (ν) and temperature (T) difference of the extinction coefficient (ϵ) as the following:

$$\epsilon(\nu,T) \propto S(\nu) \exp\{-h\nu(\nu - \nu_{00})/kT\} \quad (1)$$

where ν_{00} is the wavenumber of the 0−0 transition and k is the Boltzmann constant. $S(\nu)$ is determined by the density of the vibrational states and Franck−Condon factors. Using the above model, Okazaki et. al have shown that a plot of the absorption coefficient at a particular wavelength is directly proportional to the change in temperature of the molecular thermometer.[19] A linear dependence of the change in absorption with temperature was also observed in IR-165 dye embedded in a polymer matrix.[47,48] Accordingly, the transient absorption signals discussed in this report are assumed to change linearly with temperature. Exploiting this property of the hot band absorption we can analyze the temperature change in the immediate vicinity of the molecular heater. The temperature attained by the heater molecule can be estimated from the decay curve of transient absorption at the wavelengths corresponding to the hot band of ATC.

To correlate the transient time profile with the temporal change of the molecular temperature the amplitude of the initial temperature spike was estimated assuming that upon excitation the excess energy quickly redistributes over all vibrational modes of the Az-Pro-ATC complex. According to a thermal Boltzmann distribution, the initial internal temperature can be derived from the following:

$$E_{ph} = \sum_i \frac{\hbar\omega_i}{1 - \exp(-\hbar\omega_i/kT)} - E(T_0) \quad (2)$$

where E_{ph} is the energy of the exciting photon, $E(T_0)$ is the internal energy of the molecule at room temperature, ω_i is a vibrational frequency, and i runs over all $3N - 6$ vibrational modes of the molecule with N atoms.

The vibrational frequencies were calculated by means of the Gaussian 98 package using a semiempirical basis set. Dependencies of the excess energy on the temperature were calculated and plotted against temperature to estimate the initial peak value. The calculations indicate that on excitation of azobenzene the initial temperature can reach about 1000 K (Figure 9). This initial temperature corresponds to the formation of equilibrated vibrational distribution in Az-Pro-ATC within ca. 1 ps after the excitation pulse. Further change in the molecular temperature follows an exponential decay with the dominant lifetime of 5.2 ps. As a result, the temperature goes down to 400 K within ca. 10 ps and reaches 300 K in about 30 ps.

In conclusion, we have studied the picosecond dynamics of an Az-Pro-ATC molecular heater (Az)−thermometer−(ATC) integrated system in THF initially excited into the S_1 state by a 100 fs laser pulse at 480 nm. By monitoring the transient absorption signal at the wavelength corresponding to the hot band of the molecular thermometer, we observed three major stages of vibrational cooling of Az-Pro-ATC. Based on our results we propose the following mechanism for the energy transfer from initially excited solute to its environment: (i) Shortly after the excitation (in ca. 0.25 ps), the S_1 state of azobenzene decays to form an initial vibrationally excited nonthermalized ground state of Az-Pro-ATC that involves vibrational modes of both azobenzene and coumarin. This hot ground state decays into a predominantly thermalized state by redistributing the energy within the molecule in ca. 0.3 ps. (ii) This thermally equilibrated state cools by transferring its energy to the closest solvent molecules (directly energy accepting (DEA) solvent shell) in 5 ps. (iii) The energy diffuses from the DEA shell into the bulk solvent in 13 ps. A model of the strong coupling between the heater and the thermometer parts of our integrated system was used to interpret the experimental data. This model implies that the temperature measured by the ATC molecular thermometer relates to the temperature of the integrated system as a whole rather than to the solvent temperature in the immediate vicinity of the thermometer. Nevertheless, the use of a heater−thermometer system linked through a relatively rigid bridge has some advantages. First, the linear dependence of the hot band absorption coefficient molecular thermometer of choice on temperature established in early works simplifies the temperature calibration and reading. Second, it allows one to determine the distance from the heater in its close proximity where temperature measurements are taken. If the thermal coupling through the bridge can be reduced, then the temperature of the solvent can be measured.

Acknowledgment. This work was conducted at the Ohio Laboratory for Kinetic Spectrometry at Bowling Green State University. NIH Grant CA 91027 is gratefully acknowledged for financial support.

References and Notes

(1) Seilmeier, A.; Scherer, P. O. J.; Kaiser, W. *Chem. Phys. Lett.* **1984**, *105*, 140.
(2) Gottfried, N. H.; Seilmeier, A.; Kaiser, W. *Chem. Phys. Lett.* **1984**, *111*, 326.
(3) Wild, W.; Seilmeier, A.; Gottfried, N. H.; Kaiser, W. *Chem. Phys. Lett.* **1985**, *119*, 259.
(4) Terazima, M. *Bull. Chem. Soc. Jpn.* **2001**, *74*, 595.
(5) Liu, J.-Y.; Fan, W.-H.; Han, K.-L.; Xu, D.-L.; Lou, N.-Q. *J. Phys. Chem. A* **2003**, *107*, 1914.
(6) Elsaesser, T.; Kaiser, W. *Annu. Rev. Phys. Chem.* **1991**, *42*, 83.
(7) Lian, T.; Locke, B.; Kholodenko, Y.; Hochstrasser, R. M. *J. Phys. Chem.* **1994**, *98*, 11648.
(8) Wondrazek, F.; Seilmeier, A.; Kaiser, W. *Chem. Phys. Lett.* **1984**, *104*, 121.
(9) Laermer, F.; Elsaesser, T.; Kaiser, W. *Chem. Phys. Lett.* **1989**, *156*, 381.
(10) Seilmeier, A.; Maier, J. P.; Wondrazek, F.; Kaiser, W. *J. Phys. Chem.* **1986**, *90*, 104.
(11) Dea'k, J. C.; Pang, Y.; Sechler, T. D.; Wang, Z.; Dlott, D. D. *Science* **2004**, *306*, 473.
(12) Elles, C. G.; Cox, M. J.; Crim, F. F. *J. Chem. Phys.* **2004**, *120*, 6973.
(13) Iwaki, L. K.; Dlott, D. D. *J. Phys. Chem.* A **2000**, *104*, 9101.
(14) Sension, R. J.; Repinec, S. T.; Szarka, A. Z.; Hochstrasser, R. M. *J. Chem. Phys.* **1993**, *98*, 6291.

(15) Schwarzer, D.; Troe, J.; Votsmeier, M.; Zerezke, M. *J. Chem. Phys.* **1996**, *105*, 3121.
(16) Schwarzer, D.; Troe, J.; Votsmeier, M.; Zerezke, M. *J. Chem. Phys.* **1997**, *107*, 8380.
(17) Yamaguchi, T.; Kimura, Y.; Hirota, N. *J. Chem. Phys.* **2000**, *113*, 2772.
(18) Okazaki, T.; Hirota, N.; Nagata, T.; Osuka, A.; Terazima, M. *J. Am. Chem. Soc.* **1999**, *121*, 5079.
(19) Okazaki, T.; Hirota, N.; Nagata, T.; Osuka, A.; Terazima, M. *J. Phys. Chem.* **1999**, *103*, 9591.
(20) Rau, H. In *Photochromism: Molecules and Systems*; Durr, H., Bouas-Laurent, H., Eds.; Elsevier: Amsterdam, Boston, 2003; p 165.
(21) Ikeda, T.; Tsutsumi, O. *Science* **1995**, *268*, 1873.
(22) Shipway, A. N.; Willner, I. *Acc. Chem. Res.* **2001**, *34*, 421.
(23) Ballardini, R.; Balzani, V.; Credi, A.; Gandolfi, M. T.; Venturi, M. *Acc. Chem. Res.* **2001**, *34*, 445.
(24) Balzani, V.; Credi, A.; Venturi, M. *Coord. Chem. Rev.* **1998**, *171*, 3.
(25) Rau, H. *J. Photochem.* **1984**, *26*, 221.
(26) Rau, H.; Luddecke, E. *J. Am. Chem. Soc.* **1982**, *104*, 1616.
(27) Okamoto, H.; Hamaguchi, H.; Tasumi, M. *Chem. Phys. Lett.* **1986**, *130*, 185.
(28) Curtis, R. D.; Hilborn, J. W.; Wu, G.; Lumsden, M. D.; Wasylishen, R. E.; Pincock, J. A. *J. Phys. Chem.* **1993**, *97*, 1856.
(29) Rau, H. *Angew. Chem., Int. Ed. Engl.* **1973**, *12*, 224.
(30) Biswas, N.; Umapathy, S. *Chem. Phys. Lett.* **1995**, *234*, 24.
(31) Armstrong, D. R.; Clarkson, J.; Smith, W. E. *J. Phys. Chem.* **1995**, *99*, 17825.
(32) Morgante, C. G.; Struve, W. S. *Chem. Phys. Lett.* **1979**, *68*, 267.
(33) Lednev, I. K.; Ye, T.-Q.; Hester, R. E.; Moore, J. N. *J. Phys. Chem.* **1996**, *100*, 13338.
(34) Hamm, P.; Ohline, S. M.; Zurek, M.; Roshinger, T. *Laser Chem.* **1999**, *19*, 45.
(35) Hamm, P.; Ohline, S. M.; Zinth, W. *J. Chem. Phys.* **1997**, *106*, 519.
(36) Terazima, M.; Takezaki, M.; Yamaguchi, S.; Hirota, N. *J. Chem. Phys.* **1998**, *109*, 603.
(37) Gentili, P. L.; Danilov, E. O.; Ortica, F.; Rodgers, M. A. J. *Photochem. Photobiol. Sci.* **2004**, *3*, 886.
(38) Frisch, M. J.; Trucks, G. W.; Schlegel, H. B.; Scuseria, G. E.; Robb, M. A.; Cheeseman, J. R.; Zakrzewski, V. G.; Montgomery, J. A., Jr.; Stratmann, R. E.; Burant, J. C.; Dapprich, S.; Millam, J. M.; Daniels, A. D.; Kudin, K. N.; Strain, M. C.; Farkas, O.; Tomasi, J.; Barone, V.; Cossi, M.; Cammi, R.; Mennucci, B.; Pomelli, C.; Adamo, C.; Clifford, S.; Ochterski, J.; Petersson, G. A.; Ayala, P. Y.; Cui, Q.; Morokuma, K.; Malick, D. K.; Rabuck, A. D.; Raghavachari, K.; Foresman, J. B.; Cioslowski, J.; Ortiz, J. V.; Stefanov, B. B.; Liu, G.; Liashenko, A.; Piskorz, P.; Komaromi, I.; Gomperts, R.; Martin, R. L.; Fox, D. J.; Keith, T.; Al-Laham, M. A.; Peng, C. Y.; Nanayakkara, A.; Gonzalez, C.; Challacombe, M.; Gill, P. M. W.; Johnson, B. G.; Chen, W.; Wong, M. W.; Andres, J. L.; Head-Gordon, M.; Replogle, E. S.; Pople, J. A. *Gaussian 98*, revision A.6; Gaussian, Inc.: Pittsburgh, PA, 1998.
(39) Becke, A. D. *J. Chem. Phys.* **1993**, *98*, 5648.
(40) Lee, C.; Yang, W.; Parr, R. G. *Phys. Rev.* **1988**, *B37*, 785.
(41) Becke, A. D. *J. Chem. Phys.* **1988**, *88*, 1053.
(42) Kohn, W.; Sham, L. J. *Phys. Rev.* **1965**, *140*, A1133.
(43) Lednev, I. K.; Ye, T.-Q.; Matousek, P.; Towrie, M.; Foggi, P.; Neuwahl, F. V. R.; Umapathy, S.; Hester, R. E.; Moore, J. N. *Chem. Phys. Lett.* **1998**, *290*, 68.
(44) Nägele, T.; Hoche, R.; Zinth, W.; Wachtveil, J. *Chem. Phys. Lett.* **1997**, *272*, 489.
(45) Nofal, Z. M.; El-Zahar, M. I.; Abd El-Karim, S. S. *Molecules* **2000**, *5*, 99.
(46) Kovalenko, S. A.; Schanz, R.; Hennig, H.; Ernsting, N. P. *J. Chem. Phys.* **2001**, *115*, 3256.
(47) Wen, X.; Tolbert, A.; Dlott, D. D. *Chem. Phys. Lett.* **1992**, *192*, 315.
(48) Wen, X.; Tolbert, A.; Dlott, D. D. *J. Chem. Phys.* **1993**, *99*, 4140.
(49) Satzger, H.; Root, C.; Braun, M. *J. Phys. Chem. A* **2004**, *108*, 6265.
(50) Fujino, T.; Arzhantsev, S. Yu.; Tahara, T. *Bull. Chem. Soc. Jpn.* **2002,** *75*, 1031.
(51) Graham, P. B.; Matus, K. J. M.; Stratt, R. M. *J. Chem. Phys.* **2004**, *121*, 5348.
(52) Deng, Y.; Ladanyi, B. M.; Stratt, R. M. *J. Chem. Phys.* **2002**, *117*, 10752.
(53) Deng, Y.; Stratt, R. M. *J. Chem. Phys.* **2002**, *117*, 1735.
(54) Okazaki, T.; Hirota, N.; Terazima, M. *J. Chem. Phys.* **1999**, *110*, 11399.
(55) Seilmeier, A.; Kaiser, W. In *Ultrashort Laser Pulses and Applications*, 2nd ed.; Kaiser, W., Ed.; Springer-Verlag: New York, 1993.